Journal of Cranio-Maxillo-Facial Surgery 47 (2019) 204–218

Contents lists available at ScienceDirect

Journal of Cranio-Maxillo-Facial Surgery

journal homepage: www.jcmfs.com

Computer-assisted surgery in therapeutic strategy distraction osteogenesis of hemifacial microsomia: Accuracy and predictability

Andy Tan [a, 1], Yuanhao Chai [b, 1], Weijun Mooi [a], Xiaojun Chen [a], Haisong Xu [a], Mar Aung Zin [a], Li Lin [a], Yan Zhang [a], Xianxian Yang [a, *], Gang Chai [a, c, d, **]

[a] Department of Plastic and Reconstructive Surgery, Shanghai Ninth People's Hospital, Shanghai JiaoTong University School of Medicine, China
[b] Sonoma Academy, 2500 Farmers Lane, Santa Rosa, CA, 95404, USA
[c] Medical Device College, Shanghai University of Medicine and Health Sciences, No. 257, Zhouzhu Highway, Pudong District, Shanghai, China
[d] Department of Plastic and Reconstructive Surgery, Maternal and Child Health Care Hospital of Hainan Province, Haikou 570206, China

A R T I C L E I N F O

Article history:
Paper received 27 June 2018
Accepted 16 November 2018
Available online 6 December 2018

Keywords:
Computer-assisted surgery
Virtual surgical planning
Hemifacial microsomia
Distraction osteogenesis
Accuracy

A B S T R A C T

Background: Distraction osteogenesis can be used to treat hemifacial microsomia in patients of any age group. Application of three-dimensional (3D) technology in the surgical planning of distraction osteogenesis allows the placement of an intraoral distractor to define the cutting line and help predict the outcome of surgery.

Aim: This study compared the results of distraction osteogenesis performed, using computer-assisted surgery, on OMENS-plus-classified M2A, M2B, and M3 type patients. Comparisons were in terms of either accuracy or predictability.

Methods: 40 patients were selected to participate in the 8-month study. Preoperative image data from 3D-CT scans of the 40 patients were translated into DICOM format 3D cephalometrics, run using the computer software MIMICS version 18, and based on eight reference anatomical landmark points, five lines of measurement, and the midline of the mandibular plane. The distraction vector for the affected side of mandible was selected and the elongation process simulated repeatedly until satisfactory results were obtained. The surgical guide was created using CAD/CAM-RP technology. The distraction osteogenesis procedure was then performed using the surgical guides. Follow-up for all patients continued until 8 months postoperatively. Accuracy with and without computer-assisted surgery was assessed linearly and volumetrically. Simple mean comparisons and paired t-tests were conducted using IBM SPSS V21.

Results: In those patients who received computer-assisted surgery, distraction in the M2A type mandible showed accuracy of around 97.77% ± 7.92% ($p > 0.05$) for height and 97.91% ± 10.23% ($p > 0.05$) for length of the mandible. Meanwhile, the M2B type mandible presented accuracy of around 93.85% ± 8.07% ($p > 0.05$) for height and 95.85% ± 10.16% ($p > 0.05$) for length. For the M3 type mandible accuracy was around 98.42% ± 6.58% ($p > 0.05$) for height and 97.14% ± 11.45% ($p > 0.05$) for length. These measurements showed no significant differences between preoperative design and real outcome.

Conclusions: Individualized guides improve the accuracy of distraction osteogenesis. They help the surgeon to identify the mandibular defect and ensure the desired outcome after the operation.

1. Introduction

Since McCarthy successfully applied the distraction osteogenesis technique to mandibular lengthening on hemifacial microsomia (HFM) patients in 1992, distraction osteogenesis has played an important role because of its simplicity and consequent reduction in surgery time and donor site morbidity (McCarthy et al.,

* Corresponding author. Department of Plastic and Reconstructive Surgery; Shanghai Ninth People's Hospital, 639 Zhi Zao Ju Road, 200011, Shanghai, China.
** Corresponding author. Department of Plastic and Reconstructive Surgery, Shanghai Ninth People's Hospital, 639 Zhi Zao Ju Road, 200011, Shanghai, China.
E-mail addresses: daisywisdom8@hotmail.com (X. Yang), 13918218178@163.com (G. Chai).
[1] Andy Tan and Yuanhao Chai are co-first authors and contributed equally to the work.

https://doi.org/10.1016/j.jcms.2018.11.014
1010-5182/

1992, 2001). At the time he proposed an external distractor. Intraoral distractors subsequently developed that were less invasive but more challenging, with the level of difficulty increasing as the technique evolved.

With the development of medical technology, especially in three-dimensional imaging (3D-CT scanning and MRI), 3D cephalometry software, CAD/CAM technology, and medical analysis software, the treatment of HFM has become more advanced, predictable, and accurate, with fewer complications (Troulis et al., 2002; Gateno et al., 2011; Grayson et al., 1988). Application of 3D technology in the surgical planning of distraction osteogenesis allows the placement of an intraoral distractor to define the cutting line and help predict the outcome of surgery. Rapid prototyping technology or 3D printing is now often used to individualize the surgical guide. 3D models can be printed, and simulation can be performed to achieve a better surgical outcome, both functionally and aesthetically.

This study compared the results of distraction osteogenesis performed, using computer-assisted surgery, on OMENS-plus-classified M2A, M2B, and M3 type patients. Comparisons were in terms of either accuracy or predictability. It was hypothesized that distraction osteogenesis performed by this technique produces the same results as predicted by computer simulation.

2. Material and methods

2.1. Subjects

40 patients were randomly selected from those admitted to the Plastic and Reconstructive Surgery Department of Shanghai Ninth People's Hospital, who were diagnosed with unilateral HFM between June 2015 and October 2016. All 40 patients participated in this 8-month study, and were inpatients for the treatment of HFM using distraction osteogenesis. Inclusion criteria were as follows: patients with diagnosis of unilateral HFM; age between 2 and 9 years old; diagnosis of M2A, M2B, and M3 type, using the OMENS-plus classification; preoperative and postoperative 3D-CT scan imaging data available; good oral hygiene; good conditions of health and nutrition; and patients with informed consent. Exclusion criteria were as follows: patients with bad family compliance; those with a diagnosis of bilateral HFM.

Table 1
Three-dimensional cephalometric reference points (anatomical landmarks).

Reference points (anatomical landmarks)	Definition
Anterior nasal spine (ANS)	Highest point on nasal spine
Condylar left (CoL)	Most posterior and superior point on the left side of the mandibular condyle
Condylar right (CoR)	Most posterior and superior point on the left side of the mandibular condyle
Gonion left (GoL)	Most posterior and inferior point on the left side of the curve between the body and ascending ramus of the mandible
Gonion right (GoR)	Most posterior and inferior point on the right side of the curve between the body and ascending ramus of the mandible
Menton (Men)	Most inferior and anterior point of the mental region
Pogonion (Pog)	Most anterior point of the mental symphysis
Point B	The deepest point of the mandibular alveolar concavity

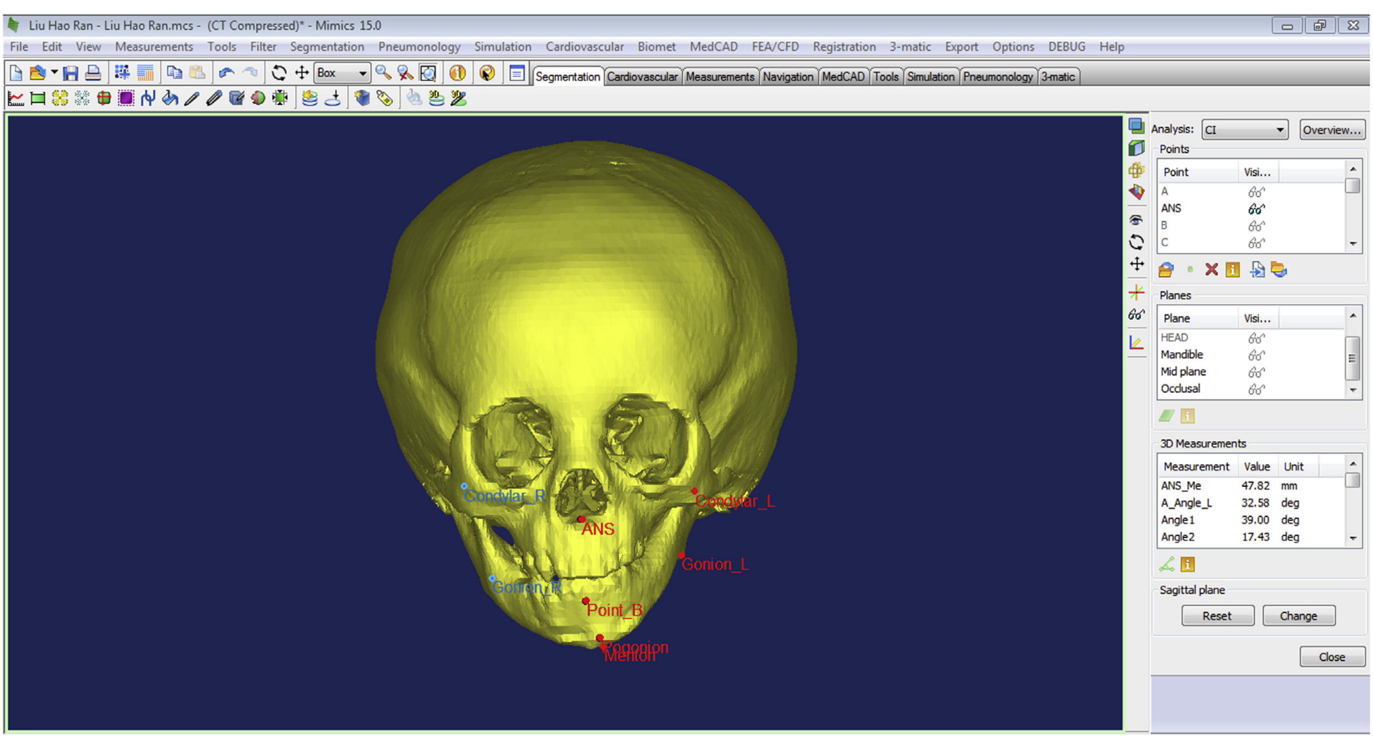

Fig. 1. Three-dimensional cephalometric image with landmarks.

3. Methods

3.1. 3D data acquisition and cephalometric analysis

All 40 patients underwent preoperative, full craniofacial, 3D-CT scanning (64-slice; Somatom Definition Flash 80 kV, Siemens). Data were collected in DICOM format (Digital Imaging and Communication in Medicine), to be rendered into 3D images. The same procedure was repeated in patients after distractor removal and within 2 weeks after the surgical procedure.

DICOM data from the medical imaging were processed using 3D analysis software (MIMICS V18, Materialise N.V., Leuven, Belgium). This involved a reorientation of the 3D-CT scan data, segmentation of the anatomical components (skull, mandible, and maxilla) and the establishment of a composite model combining all necessary information via registration.

3D cephalometric reference points (anatomical landmarks) for further facial skeleton analysis are listed in Table 1 and shown in Fig. 1. These reference points were applied to three kinds of 3D model (preoperative, virtual surgical, and postoperative). The 3D data were applied to our assessment method (Table 2), which was used to measure and classify patients within each group according to the OMENS-plus classification system. The software was able to calibrate the measurement.

Table 2
Measurement standards for the assessment of 3D data.

No	Measurement	Definition
1	ANS-Men (mm)	Distance from anterior nasal spine to menton. This represents anterior lower facial height.
2	CoL–CoR (mm)	Linear distance from left condyle to right condylar. This represents inter-temporomandibular-joint distance.
3	CoL–GoL (mm)	Linear distance from condyle to gonion on left side of mandible. This represents left mandibular ramus height.
4	CoR–GoR (mm)	Linear distance from condyle to gonion on right side of mandible. This represents right mandibular ramus height.
5	GoL–GoR (mm)	Linear distance from left gonion to right gonion. This represents width of mandible.
6	GoL–Pog (mm)	Linear distance from left gonion to pogonion. This represents length of left mandibular body.
7	GoR–Pog (mm)	Linear distance from right gonion to pogonion. This represents length of right mandibular body.
8	Gonion angle L (deg)	Angle formed by left condyle, left gonion, and pogonion. This represents left mandibular angle.
9	Gonion angle R (deg)	Angle formed by right condyle, right gonion, and pogonion. This represents right mandibular angle.

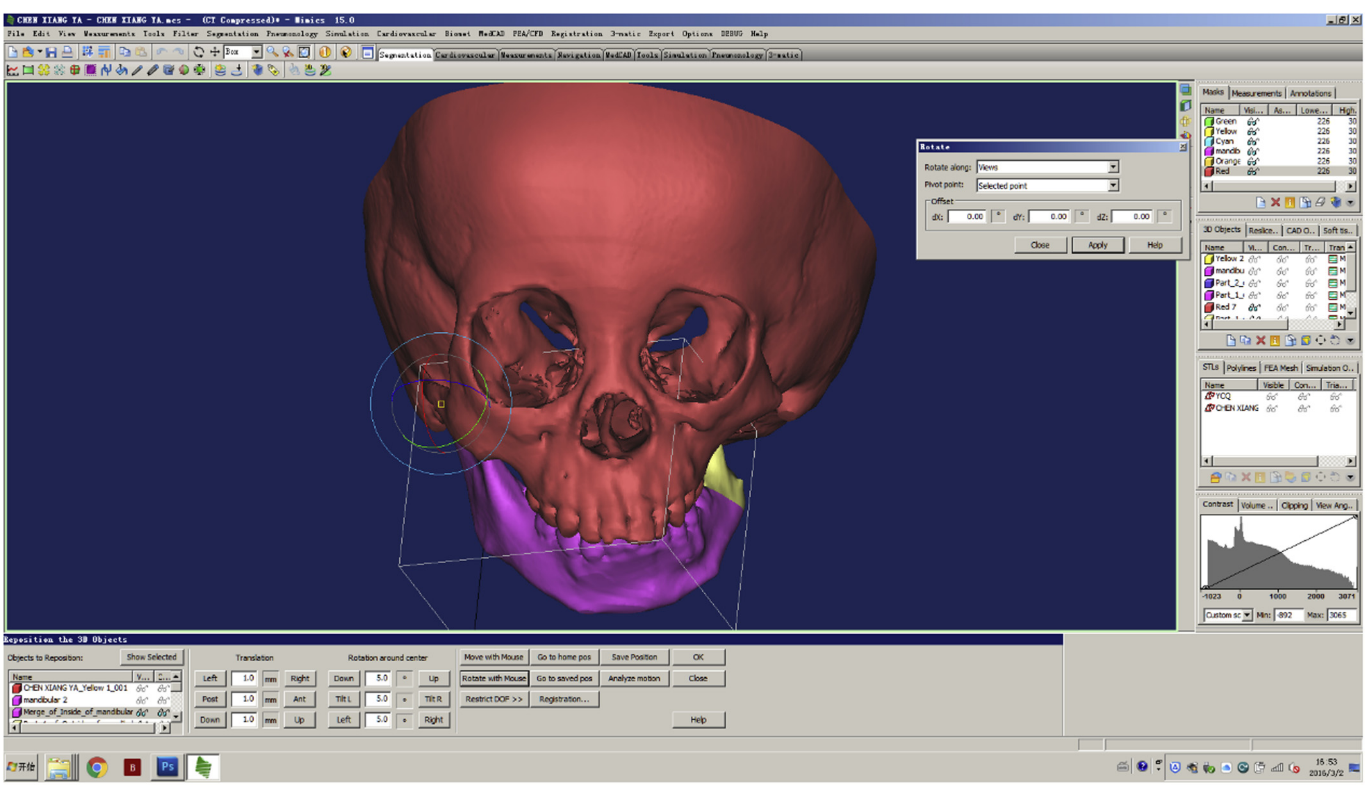

Fig. 2. MIMICS V8 simulation of the surgery process in order to predict the result of surgery (front view). The starting pivot point is the non-affected side condyle, with the predicted osteotomy line established by computer simulation.

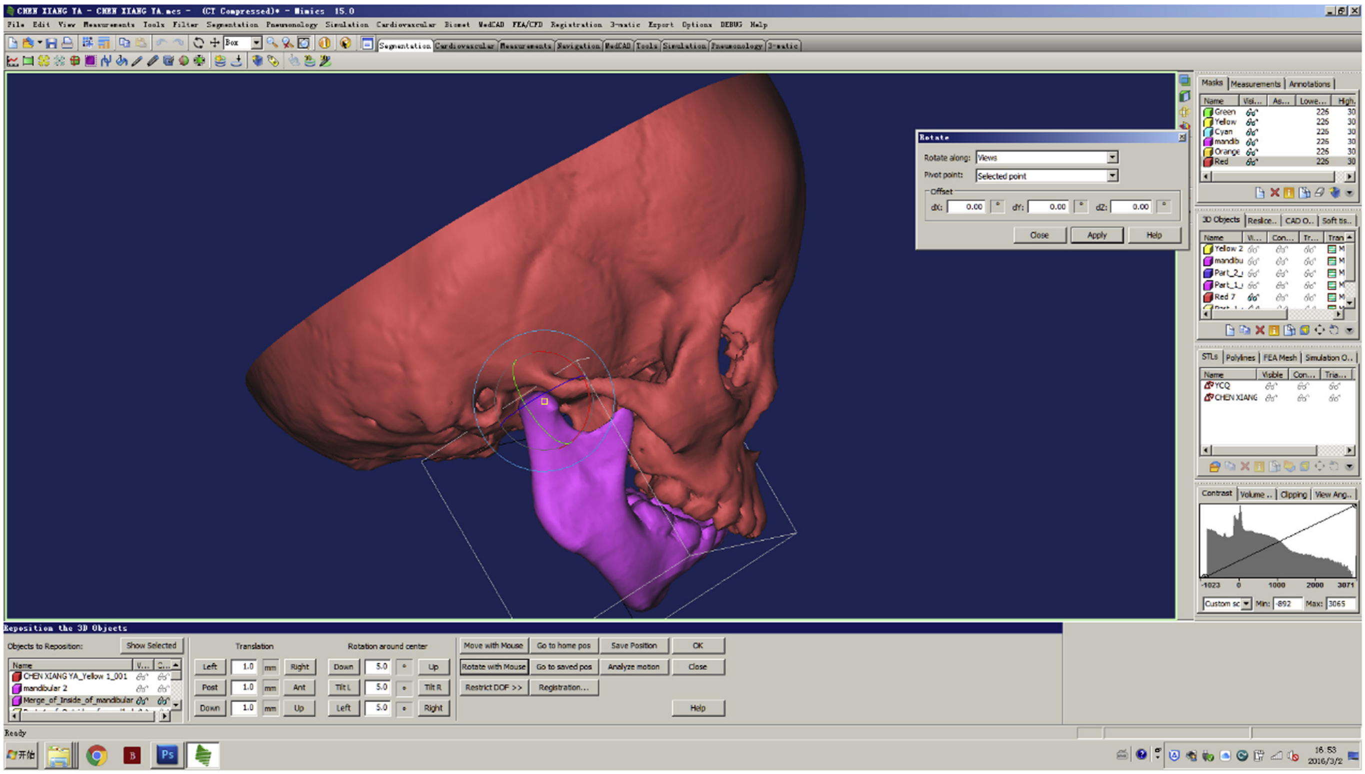

Fig. 3. MIMICS V8 simulation of the surgery process in order to predict the result of surgery (side view). The right condyle is used as a pivot point to simulate the mandible distraction process.

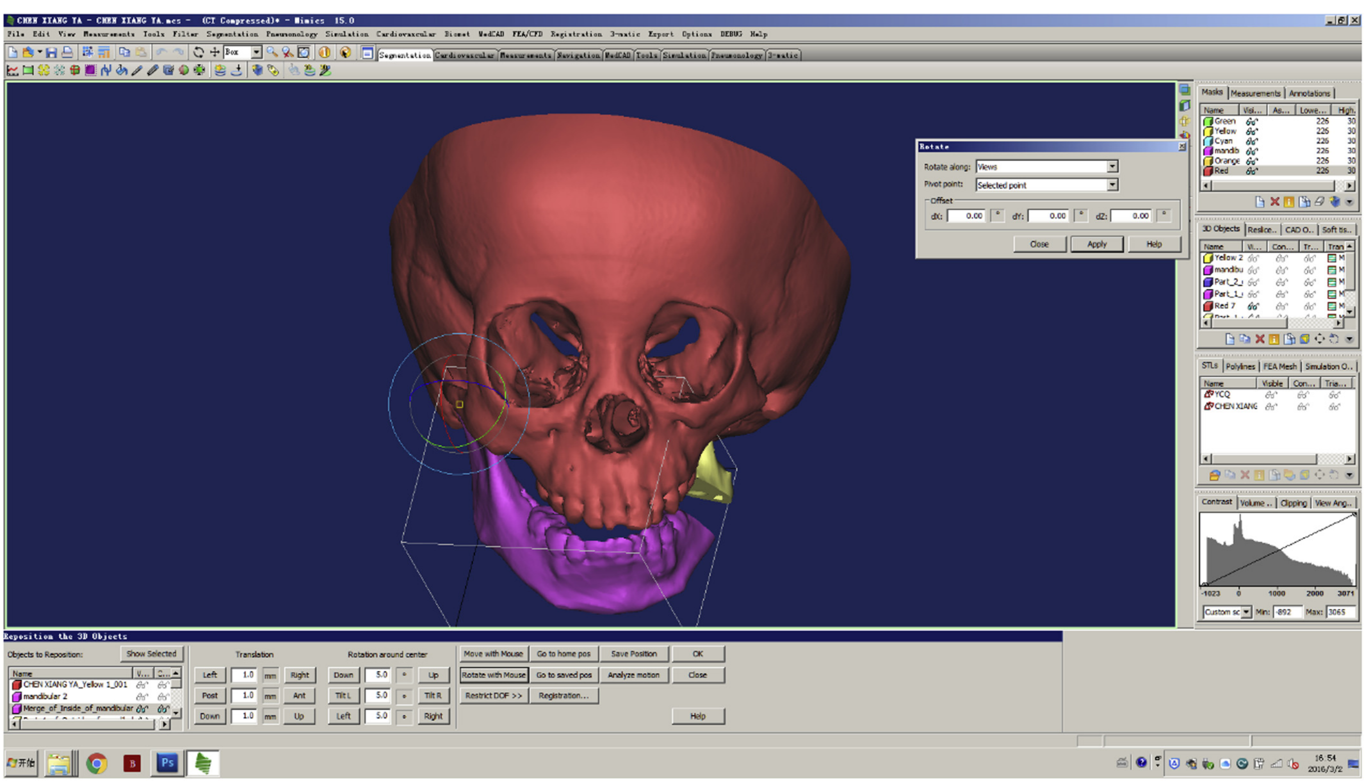

Fig. 4. MIMICS V8 simulation of the surgery process in order to predict the result of surgery (front view, showing the result of the mandible distraction process). The mandible is distracted until the pogonion is through the midline or sagittal line. The occlusal plane downright and near to normal data.

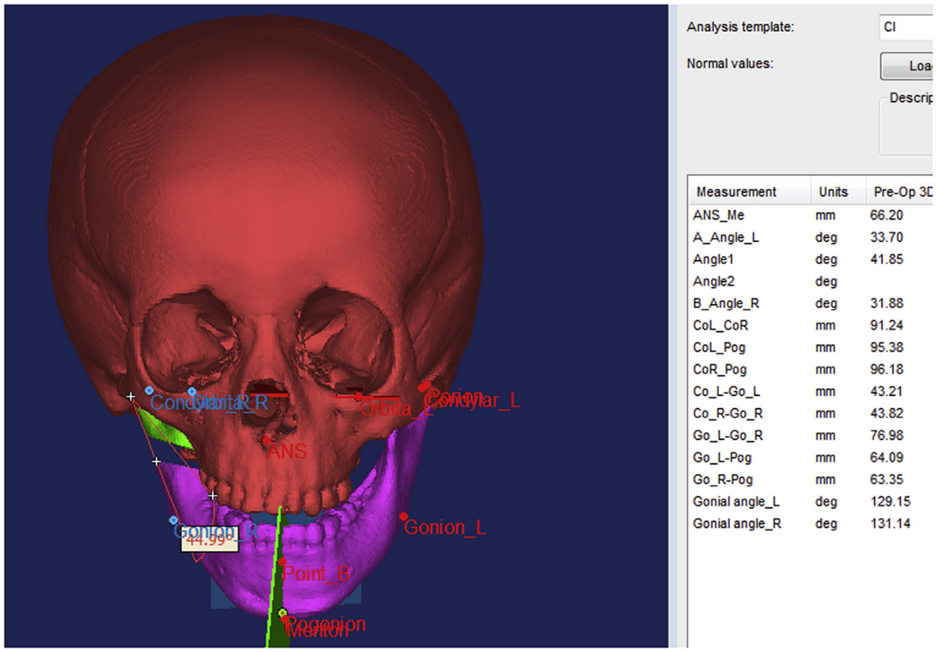

Fig. 5. Measurement and analysis for each parameter value. The table to the right shows the value for each measurement.

3.2. Virtual surgical planning

The surgical simulation process was run through MIMICS V15 to predict the outcome of the surgery. The distraction vector for the affected mandible in each HFM patient was based on the maxillary occlusal plane (MOP). The imaginary osteotomy line was added and a simulation of the distraction process run repeatedly. This allowed us to predict the outcome of the distraction process. The measurements from Table 2 were also applied to these 3D simulated models. One aim was to measure the accuracy of our predictions based the simulated distraction outcome.

The first step was to input the 3D-CT DICOM into the computer software, which ran the data using an STL file extension. This STL file imported and arranged the directions of the image (top, bottom,

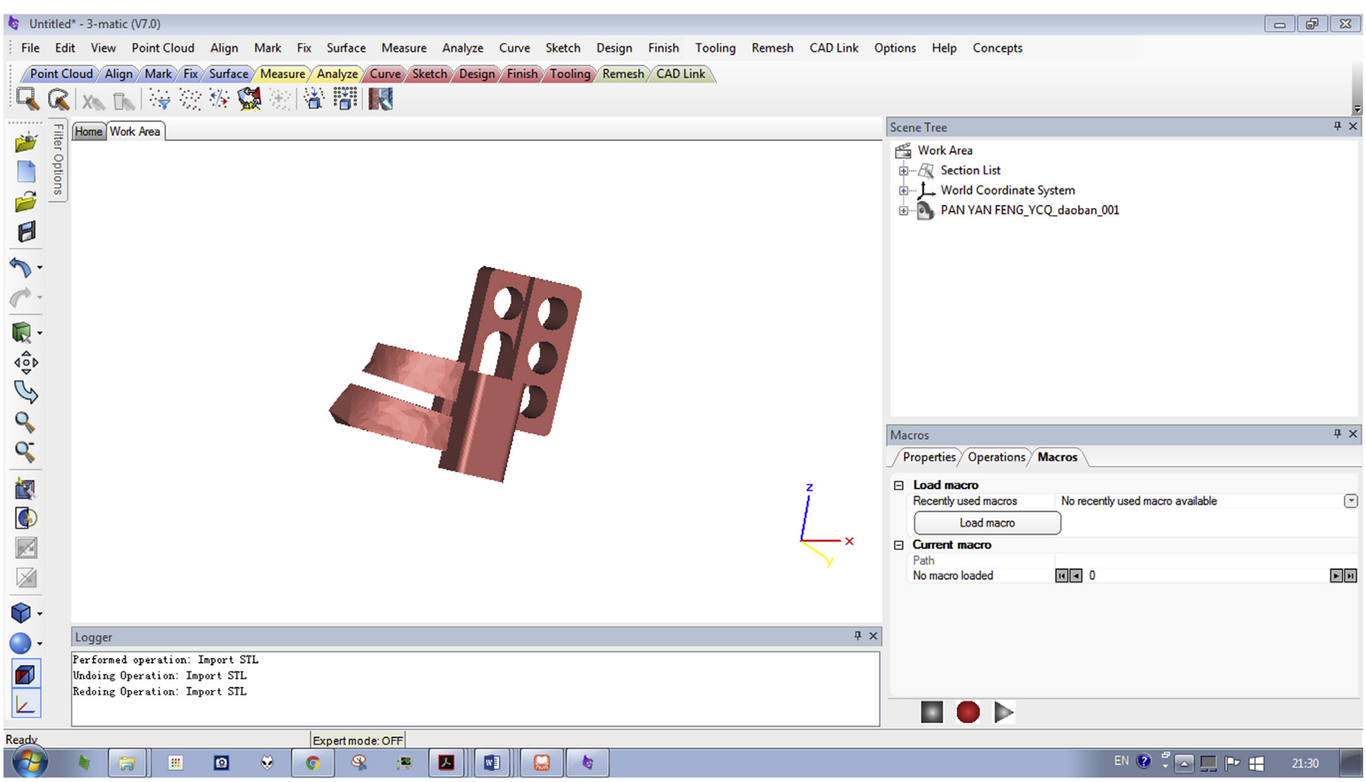

Fig. 6. Preoperative surgical guidance design to be translated intraoperatively.

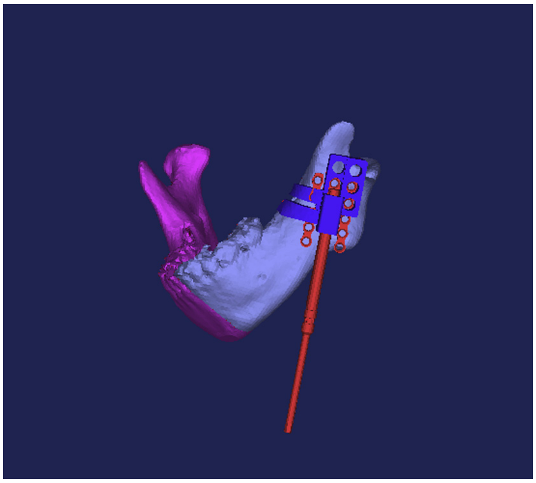

Fig. 7. Surgical guidance simulation in 3D models, with distractor.

left, right, anterior, and posterior). The segmentation process for the 3D models began by selecting the exact thresholding for the bone structure, followed by mask editing, Boolean operations, and calculation of 3D models. The second step was the simulation, in which the MIMICS software used measurement data and analysis to guide the surgical process. The cephalometric landmarks used are listed in Table 1 and shown in Fig. 1, while the measurements used for analysis are explained in Table 2.

The surgical simulation process was run repeatedly until satisfactory results were gained (Fig. 2). The main pivoting point was the non-affected mandibular condyle (Fig. 3). The mandible was reset as far as the pogonion, through the midline or sagittal line (Fig. 4). The reset mandible was then measured and analyzed, and measurement results for each parameter collected (Fig. 5).

Intraoperative guidance, such as surgical splints for the osteotomy line and intraoral distractor placement, was digitally designed using computer-aided design (CAD)/computer-aided manufacturing (CAM) software (3-Matic V7.0; Materialise, Leuven, Belgium). The simulation is shown in Fig. 6. The surgical guide was printed using rapid prototyping (RP) technology or a 3D printer, and applied intraoperatively (Fig. 7). Simulation involving 3D-printed mandible models, surgical guide, and distraction device is shown in Fig. 8.

3.3. Surgical procedure

The distraction osteogenesis procedure was performed under general anesthesia. The incision was made intraorally from the lower inferior buccal side. An injection of lidocaine 1% with 1:100 000 epinephrine was applied before the incision. The incision was made from the first molar to the biting line between upper and lower teeth, using a surgical blade 11. The periosteal (on the medial and lateral side of the mandible) was released, and hemostasis was performed to minimize blood loss during the procedure. The

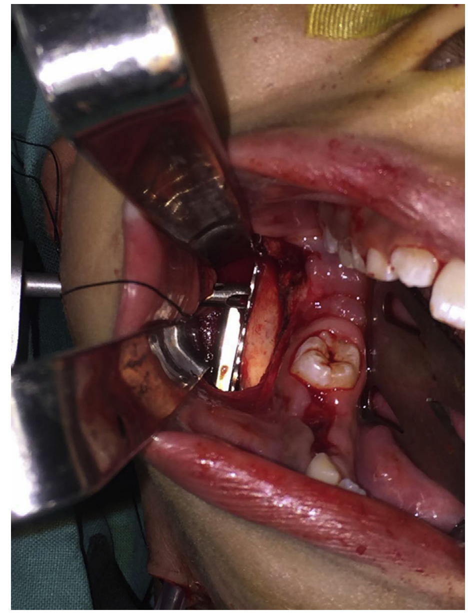

Fig. 9. Surgical guide applied intraorally during operation.

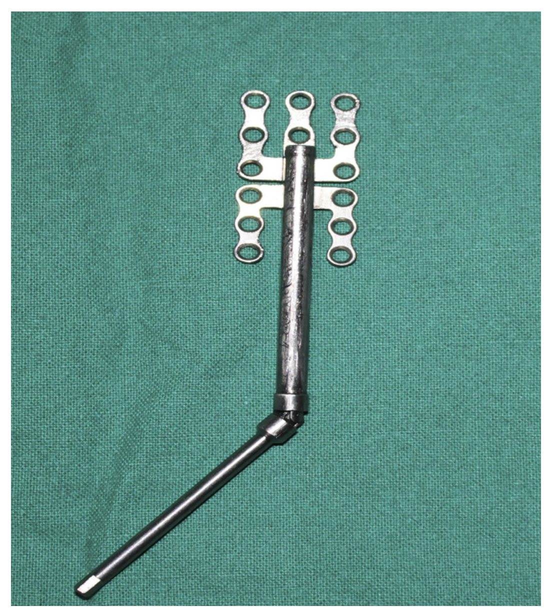

Fig. 10. The intraoral distractor device used in our department (maximum length of distraction 30 mm; Ningbo Cibei Medical Treatment Appliance Co. Ltd, China).

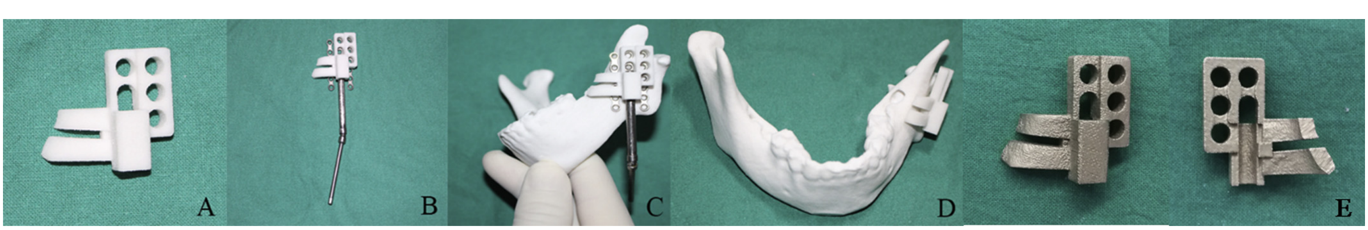

Fig. 8. A: 3D-printed intraoperative surgical guide for osteotomy line on affected mandible. B: Surgical guide with distraction device for a preoperative recheck. C: Distraction device with surgical guide placed on 3D-printed mandible models for simulation. D: Surgical guide and 3D-printed mandibular models. E: Metal surgical guide used for the operation.

surgical guide was placed above the mandibular ramus to indicate the osteotomy line (Fig. 9). The mandible was cut through the outer cortex, both medially and laterally. The inferior alveolar nerve was secured before placement of the distractor intraorally. Six screws were used to secure the distractor — three proximally and three distally — and a drain was inserted before the oral mucosa was closed using vicryl 5-0 absorbable. Fig. 10 shows the distractor used in our department.

A latency phase of around 5–7 days followed the osteotomy procedure before the distraction process was started. The activation phase started with a rate of distraction of around 1 mm/day. Our distractor device has a rate of elongation of around 0.35 mm per rotation. The distraction process was repeated twice a day (a rotation of 0.5 mm, day and night). The consolidation phase was confirmed using a posteroanteriorcephalogram, lateral cephalogram, and panoramic radiograph (Fig. 11). The distraction process was stopped after the midline of mandible had moved across the sagittal plane. The length of time for consolidation was around 12 weeks.

The distractor was removed after the distraction process was complete and bone formation was confirmed by radiography examination (anteroposterior and lateral radiographs). Lidocaine 1% with 1:100 000 epinephrine was applied to the incision site. The incision was made on the lower inferior buccal side, from the molar teeth to the biting line. The periosteal was first released from the body of the distractor in order to access the whole distractor, including the screws. After removal of the distractor, hemostasis was performed to avoid hematoma and postoperative bleeding. The cortex bone of the mandible was then examined thoroughly to verify complete growth of the distracted segments. A drain was inserted and the incision was closed in a double layer using vicryl 4.0 and 5.0 absorbable.

3.4. *Method of assessment*

All the above-measured data were analyzed using our assessment method, which was divided into linear assessment and volumetric assessment. The data were classified into three periods and labeled as follows: T1 — preoperative distraction osteogenesis; T2 — virtual surgical planning period; and T3 — 2 weeks after removal of the intraoral distractor.

3.5. *Linear assessment*

Linear assessment data involved two-dimensional measurements. These were compared among the three periods — preoperatively, virtual surgery, and postoperatively — for each OMENS-plus classification group. The parameters chosen were: intercondylar distance; height of mandibular ramus; length of mandibular body; width of mandible; and gonial angle of the affected mandible.

These parameters were compared for the preoperative, virtual surgical planning, and postoperative data. The results of the

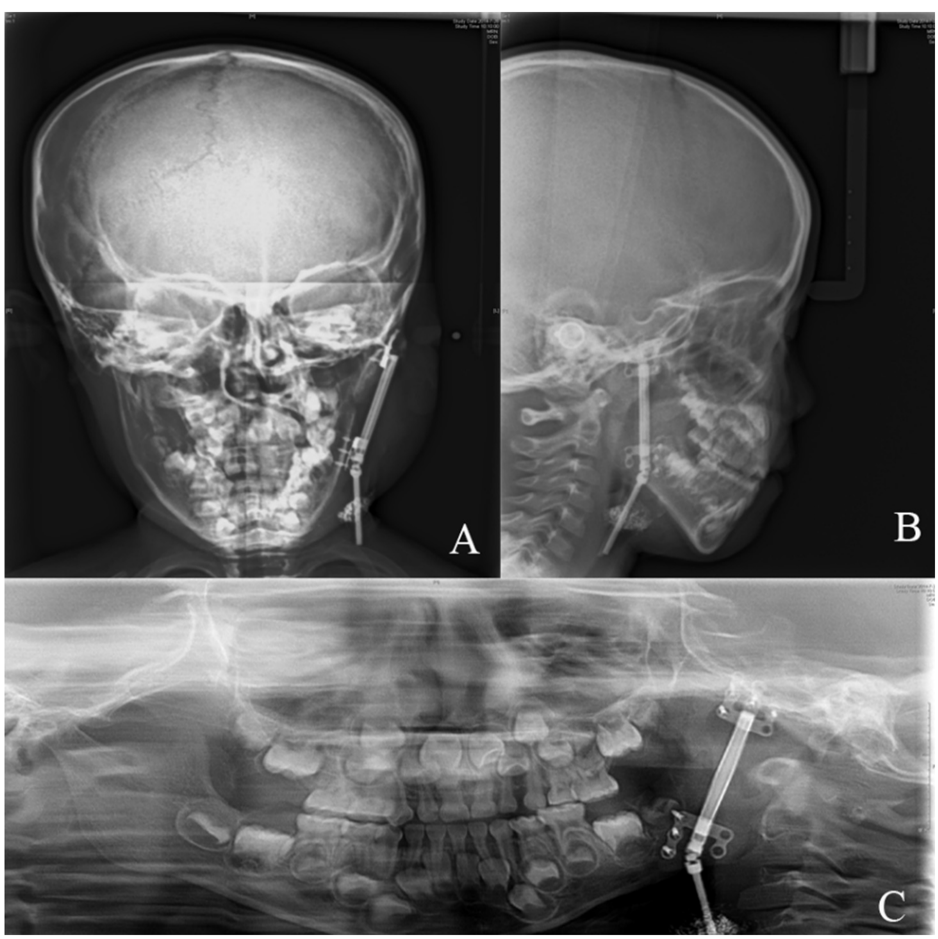

Fig. 11. A and B: Posteroanterior and lateral cephalograms of the completed distraction process for the affected mandible. C: Panoramic radiographs used to identify the occlusal plane following completion of the distraction process.

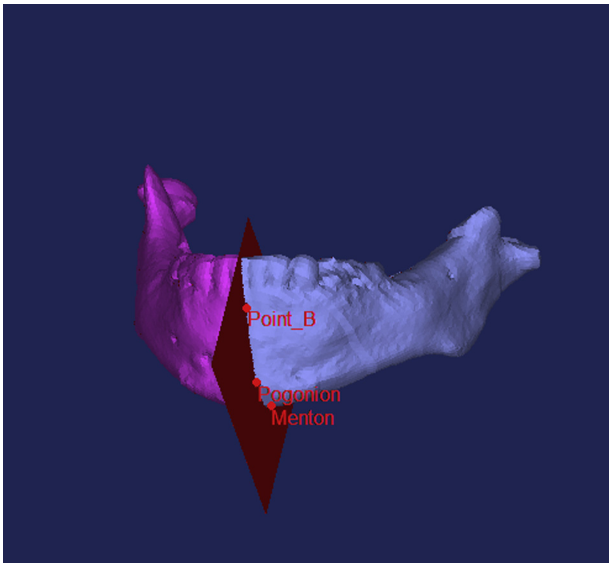

Fig. 12. Anatomical landmarks for volumetric measurement: Point-B, pogonion, and menton. Pink = non-affected side of mandible. Blue = affected side of mandible. Red plane = mandible midline plane.

Table 3
Demographic data for hemifacialmicrosomia patients.

		Frequency	Percentage (%)
Gender	Female	8	20
	Male	32	80
Age	Mean	4.46 y	
	Range	2–9 y	
Infected side	Left side	24	60
	Right side	16	40
Diagnosis	M1	0	0
	M2A	22	55
	M2B	14	35
	M3	4	15

distraction osteogenesis process and therefore the accuracy of the virtual surgical planning technique were then assessed.

Means for all the parameters were compared for each assessment period. Results of the distraction osteogenesis procedure were calculated using Equation 1. The accuracy of the virtual surgical planning distraction osteogenesis technique was calculated using Equation 2.

Equation 1:

DO result = value for each parameter from postoperative data −value for each parameter from preoperative data (Values measured in millimeters (mm))

Equation 2:

$$\text{accuracy (\%)} = [T3/T2] \times 100$$

3.6. Volumetric assessment

Volumetric measurements for the mandible were taken preoperatively and postoperatively, as well as after application of virtual surgical planning. Volumetric change was calculated by subtracting the preoperative mandibular volume from the postoperative mandibular volume. The mandible was divided into two major analysis units for volumetric analysis (non-affected side and affected side) using three anatomical landmarks (Point-B, pogonion, and menton) to create a dividing mandible midline plane (Fig. 12).

3.7. Data analysis

Data were collected and analyzed using SPSS V21. All the feature variables followed a normal distribution, so the accuracy calculations and volumetric measurements for patients were compared using group and paired t-tests. All the statistical analyses in this study set $\alpha = 0.05$, with $p < 0.05$ as statistically significant.

4. Results

All patients had unilateral HFM (24 left sided, and 16 right sided). Patients were diagnosed according to the OMENS-plus classification. The age range of the selected patients was 2–9 years, and the ratio of males and females was 4 to 1 (Table 3).

4.1. Linear measurement

Table 4 gives an overview of the three periods of the process: T1 for initial findings (preoperative); T2 for the virtually planned condition simulated by computer; and T3 for 2 weeks after surgical correction by distraction osteogenesis (postoperative). This overview includes data for all linear parameters (presented in mean and standard error form).

The linear measurement results in Table 4 represent five parameters. For each parameter, data from T2 and T3 were compared statistically using paired t-tests. The intercondylar change from preoperative (T1) to postoperative (T3) was 1.72 mm. The virtual planned (T2) measurement was 90.23 mm, giving an accuracy of around 97.78% ($p > 0.05$). The mean height of the mandibular ramus increased by 12.7 mm across all groups. The T2 measurement for height of mandibular ramus showed an accuracy of 98.82% ($p > 0.05$). Meanwhile, mandibular length increased around 3.22 mm between T1 and T3, with T2 accuracy around 98.76% ($p > 0.05$). Width increased by only 0.14 mm, giving a T2 accuracy of

Table 4
Data for each parameter for the three periods (mean ± standard deviation). The results for intercondylar changes, change in height of mandibular ramus, and change in length of mandible body are in millimeters (mm). The gonial angle is in degrees (°).

Parameter	T1	T2	T3
Intercondylar change	86.51 ± 10.42	90.23 ± 10.86	88.23 ± 10.08
Change in height of mandibular ramus	30.34 ± 8.86	43.55 ± 12.02	43.04 ± 8.99
Change in length of mandibular body	57.49 ± 7.83	61.47 ± 8.75	60.71 ± 7.99
Change in width of mandible	74.70 ± 10.11	76.47 ± 8.48	74.84 ± 10.73
Change in gonial angle of mandible	127.88 ± 16.61	140.61 ± 9.11	134.77 ± 4.05

Table 5
Measurement data for HFM type M2A for each parameter for the three time periods (mean ± standard deviation). Accuracy was calculated using Equations 1 and 2.

Linear measurement parameter	T1	T2	T3	Accuracy (%)
Intercondylar distance (mm)	88.91 ± 11.02	92.2 ± 10.91	88.77 ± 10.96	96.28
Height of mandibular ramus (mm)	34.31 ± 7.77	48.75 ± 11.57	47.66 ± 8.81	97.77
Length of mandibular body (mm)	60.01 ± 7.33	61.42 ± 9.62	60.14 ± 7.29	97.91
Width of mandibular (mm)	76.24 ± 11.31	78 ± 8.58	76.39 ± 8.82	97.94
Gonial angle of affected mandible (degrees)	129.98 ± 3.82	141.13 ± 7.08	131.20 ± 2.96	92.96

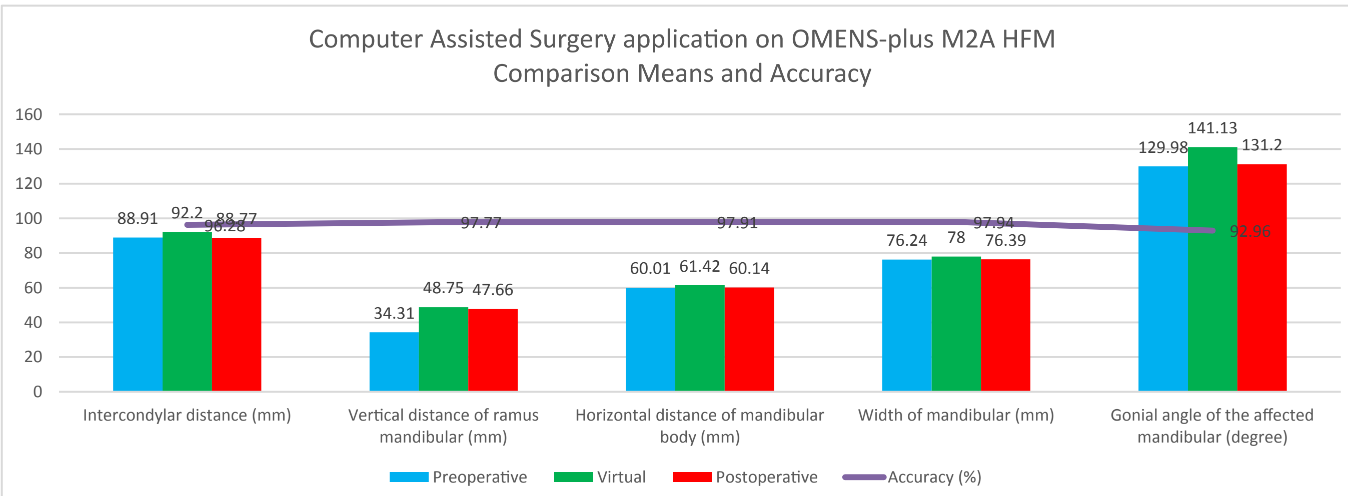

Graph 1. Computer-assisted surgery data for M2A type HFM classification: comparison of mean values for different parameters, and accuracy of simulated values.

Table 6
Measurement data for HFM type M2B for each parameter for the three time periods (mean ± standard deviation). Accuracy was calculated using Equations 1 and 2.

Linear measurement parameter	T1	T2	T3	Accuracy (%)
Intercondylar distance (mm)	87.19 ± 8.99	92.62 ± 11.05	89.16 ± 8.99	96.27
Height of mandibular ramus (mm)	28.29 ± 7.24	40.99 ± 8.05	38.47 ± 13.49	93.85
Length of mandibular body (mm)	54.84 ± 4.11	61.83 ± 10.28	59.26 ± 2.64	95.85
Width of mandibular (mm)	76.66 ± 8.28	79.15 ± 6.89	77.46 ± 8.06	97.87
Gonial angle of affected mandible (degrees)	131.69 ± 6.32	141.61 ± 11.35	136.16 ± 8.06	96.15

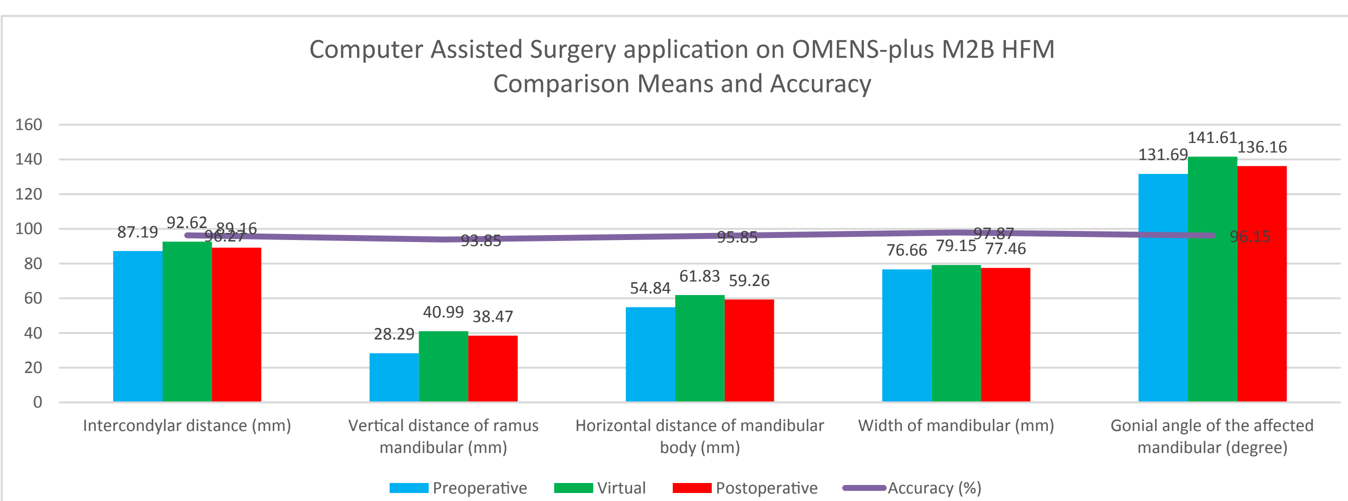

Graph 2. Computer-assisted surgery data for M2B type HFM classification: comparison of mean values for different parameters, and accuracy of simulated values.

Table 7
Measurement data for HFM type M3 for each parameter for the three time periods (mean ± standard deviation). Accuracy was calculated using Equations 1 and 2.

Linear measurement parameter	T1	T2	T3	Accuracy (%)
Intercondylar distance (mm)	84.35 ± 18.66	80.40 ± 12.08	76.44 ± 12.98	95.07
Height of mandibular ramus (mm)	15.81 ± 3.53	34.48 ± 8.78	33.94 ± 5.56	98.42
Length of mandibular body (mm)	52 ± 17.61	62.95 ± 7.36	61.15 ± 18.72	97.14
Width of mandibular (mm)	73.17 ± 6.45	74.02 ± 7.77	70.91 ± 8.62	98.13
Gonial angle of affected mandible (degrees)	112.67 ± 8.03	130.72 ± 8.41	125.16 ± 4.45	95.75

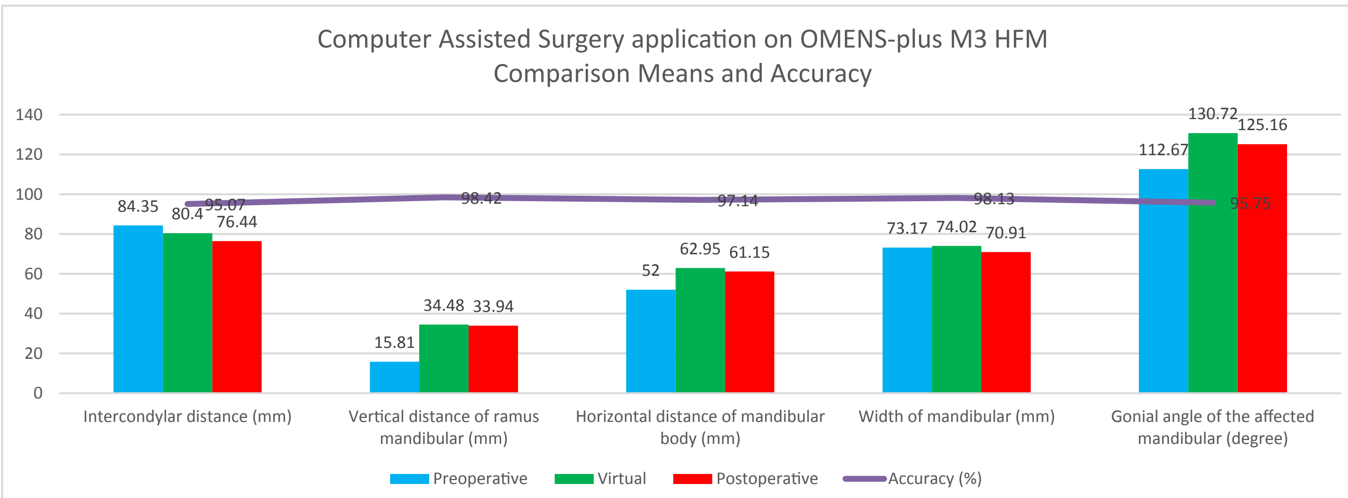

Graph 3. Computer-assisted surgery data for M3 type HFM classification: comparison of mean values for different parameters, and accuracy of simulated values.

Table 8
Comparison between preoperative and postoperative volume data.

Parameter	T1		T3		Change	
	Mean	SD	Mean	SD	Mean	SD
Volume of affected mandible	16542.11	5431.72	21944.45	5158.23	5402.34	2982.13
Volume of non-affected mandible	19779.25	6798.78	21657.42	5036.84		

97.87% ($p > 0.05$). Finally, gonial angle differed by 6.89° between T1 and T3, with T2 accuracy at around 95.84% ($p > 0.05$).

Table 5 shows the accuracy and distraction results (changes) for each parameter in the M2A type group. Comparisons of T1 and T3 data for width of mandible and gonial angle showed little change. Meanwhile, the change in height of the mandibular ramus between T1 and T3 was quite significant, at around 13.35 mm. The computer simulation for height of mandibular ramus showed an accuracy of 97.77% ($p > 0.05$). Changes in width were not significant due to the shape of the mandible. The accuracy of computer simulation was 97.91% ($p > 0.05$). Graph 1 shows the distribution of data for the M2A group.

In the M2B type mandible group, the mandible increased in height by 10.18 mm and in length by 4.42 mm The change in height in the computer simulation showed an accuracy of 93.85% ($p > 0.05$), and change in length an accuracy of around 95.85%

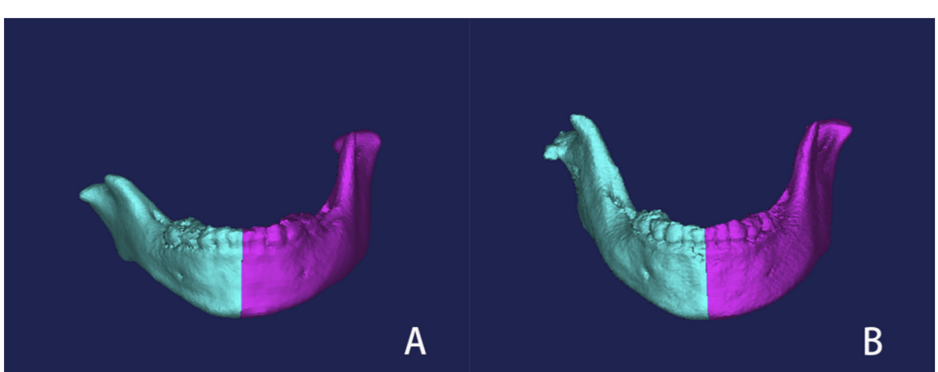

Fig. 13. A and B: Preoperative and postoperative 3D models for volumetric measurement showing non-affected side of mandible (pink) and affected side of mandible (bright blue).

Table 9
Pre- and postoperative volume data for each type of volume ratio classification.

Volume ratio classification	T1	T3	Changes
M2A	18858.98 ± 5204.01	23838.89 ± 5602.11	4979.92
M2B	16309.63 ± 5132.16	22070.79 ± 5203.14	5761.16
M3	13078.51 ± 5024.03	16818.23 ± 5130.16	3739.73

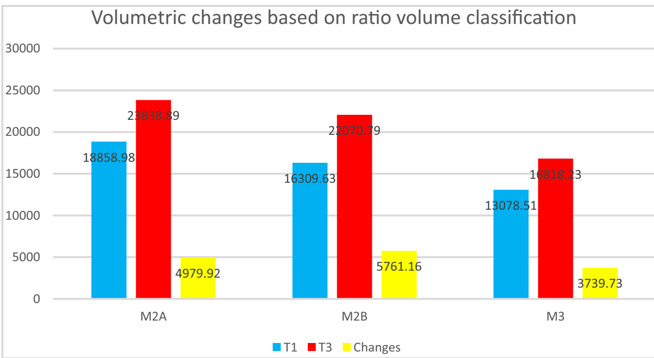

Graph 4. Volumetric changes based on volume ratio classification.

($p > 0.05$). The most significant change in this type of mandible was in the width, with an accuracy of around 97.87% ($p > 0.05$). Meanwhile, the intercondylar and gonial angle changes showed almost the same accuracy — 96.27% and 96.15%, respectively ($p > 0.05$). These data can be seen in Table 6. Graph 2 shows the distribution of data for the M2B group.

The M3 type mandible is the most severe, with no mandibular ramus and only half of the mandible body. The data for this group are shown in Table 7 and Graph 3. The computer simulation was focused on adding more volume in either the vertical or horizontal direction. The four patients in the M3 group showed an 18.13 mm gain in mandibular height and a 9.15 mm gain in length. Accuracy of the computer simulation was 98.42% ($p > 0.05$) for height and 97.14% ($p > 0.05$) for length. In spite of the good levels of accuracy for this group (95.07–98.42%), for each parameter aside from length an attempt was made to increase measurements in order to minimize secondary surgery for temporomandibular joint creation.

4.2. *Volumetric measurement*

For 3D (volumetric) measurement, we compared the volumes of both sides of the mandible (affected and non-affected) for both preoperative (T1) and postoperative (T3) stages. The data are shown in Table 8. The results of virtual distraction using the simulated technique showed an enhancement in volume of about 5402.34 mm^3, with a standard deviation (SD) of 2982.13 mm^3. The comparison of preoperative volumes for the affected side and non-affected sides showed a ratio of 1–1.2. The postoperative volume ratio for the affected and non-affected sides was 1.01 to 1 (Fig. 13). This excellent result from a volumetric point of view was confirmed statistically using a simple paired *t*-test, giving a highly significant result ($p = 0.000$).

For every type of OMENS-plus classification, the data showed significantly upright results for mean comparisons and volume changes between preoperative and post-operative stages. Enhancements in volume for all types of classification are shown in Table 9 and Graph 4.

5. Discussion

HFM is a complex dysmorphogenesis, with different phenotypes ranging widely in terms of severity. The syndrome can result in both craniofacial and extracranial abnormalities, presenting a challenge for surgeons. Facial skeletal abnormalities are an important target for correction due to their effects on soft/non-skeletal tissue growth. Experts believe that early correction of these anomalies can provide a better phenotypic outcome for HFM patients.

It was recognized early in this clinical study that in treatment planning there are several structural or architectural goals: (1) increasing the vertical dimension of the hypoplastic mandibular ramus; (2) re-establishing the transverse position of the ramus (bigonial distance) to improve cheek contour; (3) increasing the projection or anteroposterior dimension of the mandibular body and symphysis; (4) improving the dentoalveolar relations; (5) 'leveling' the occlusal plane in unilateral distraction cases; (6) correcting any asymmetry of the oral commissure (in unilateral cases); and (7) increasing (or 'overcorrecting' in the growing patient) chin projection in bilateral cases and 'overcorrecting' chin point (movement to the contralateral side) in unilateral cases.

Distraction osteogenesis was first introduced by Ilizarov, who applied it in orthopedic surgery in limb lengthening procedures. It was McCarthy, in 1992, who first applied this technique to the craniofacial field. He performed several mandibular ramus lengthening procedures in all age groups, and introduced a less-invasive technique, with lower morbidity, for correcting the mandible in HFM cases. The unique nature of this technique lay in its cutting plane and the positioning of the distractor.

It is important to predict the mandibular response preoperatively in order to maximize the benefits of this technique (Grayson et al., 1997, 1999; Hanson and Melugin, 1999). The angle formed

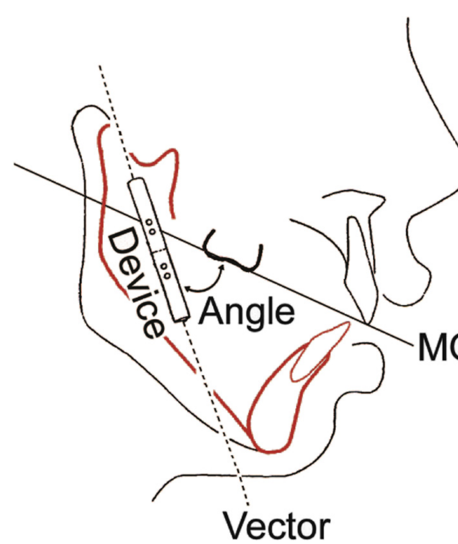

Fig. 14. The vector of distraction is defined by the angle formed between the long axis of distraction device and the maxillary occlusal plane (MOP). A horizontal vector is defined as less than 30°, an oblique vector is between 30 and 45°, and a vertical vector greater than 45°. Adapted from Dec et al. (2008).

between the long axis of the distraction device and the maxillary occlusal plane (MOP) is defined as the vector of distraction (Dec et al., 2008). The vector of distraction can be divided into three, based on direction, such as vertical, horizontal, and oblique. The horizontal vector of distraction produces marked mandibular shift but minimal elongation of the affected ramus. The vertical vector of distraction results in minimal mandibular midline shift but marked ramus elongation. The oblique vector of distraction produces an intermediate amount of ramus lengthening and a marked amount of mandibular midline shift. Longitudinal or horizontal lengthening after vector selection will determine the outcome of the surgery. It needs an experienced surgeon to achieve accurate lengthening in surgical correction, resulting in a symmetrical outcome.

Paeng et al. employed the condyle as a rotation point for vector selection in their three-dimensional planning of distraction osteogenesis for HFM (Paeng et al., 2007). With advances in technology, we can now apply CAD/CAM, 3-D printing/rapid prototyping, and virtual surgical planning software to this surgery, allowing us to predict the vector required to produce a symmetrical facial appearance (Altobelli et al., 1993; Lo et al., 1994; Eufinger et al., 1995; Cavalcanti et al., 2004).

Dec et al. emphasised the importance of vector selection in preoperative planning of unilateral mandibular distraction (Dec et al., 2008). To determine how the vector of unilateral mandibular distraction affects treatment outcomes, they divided the variable of distraction into dependent and independent variables. The dependent variable was the vector of distraction itself (Fig. 14), which was formed by the maxillary occlusal plane (MOP) and the long axis of the distraction device. The variable measurements used to assess mandibular response to the vector of distraction were percentage change in ramus length ratio, mandibular midline shift, rotation of the symphyseal plane, and movement of the pogonion. Negative correlation was found between the vector of distraction and the magnitude of the mandible midline shift. The vertical vector resulted in the greatest amount of mandibular ramal lengthening.

Clinical and surgical judgment should be taken into account when selecting the vector of distraction. The vector of distraction in our study was adjusted by the authors based in the Shanghai Ninth People's Hospital. The distraction results showed less advancement in the horizontal direction, highlighting the possibility of human error in this study. The adjustment of the distraction vector was greater in the vertical and oblique directions than in the horizontal

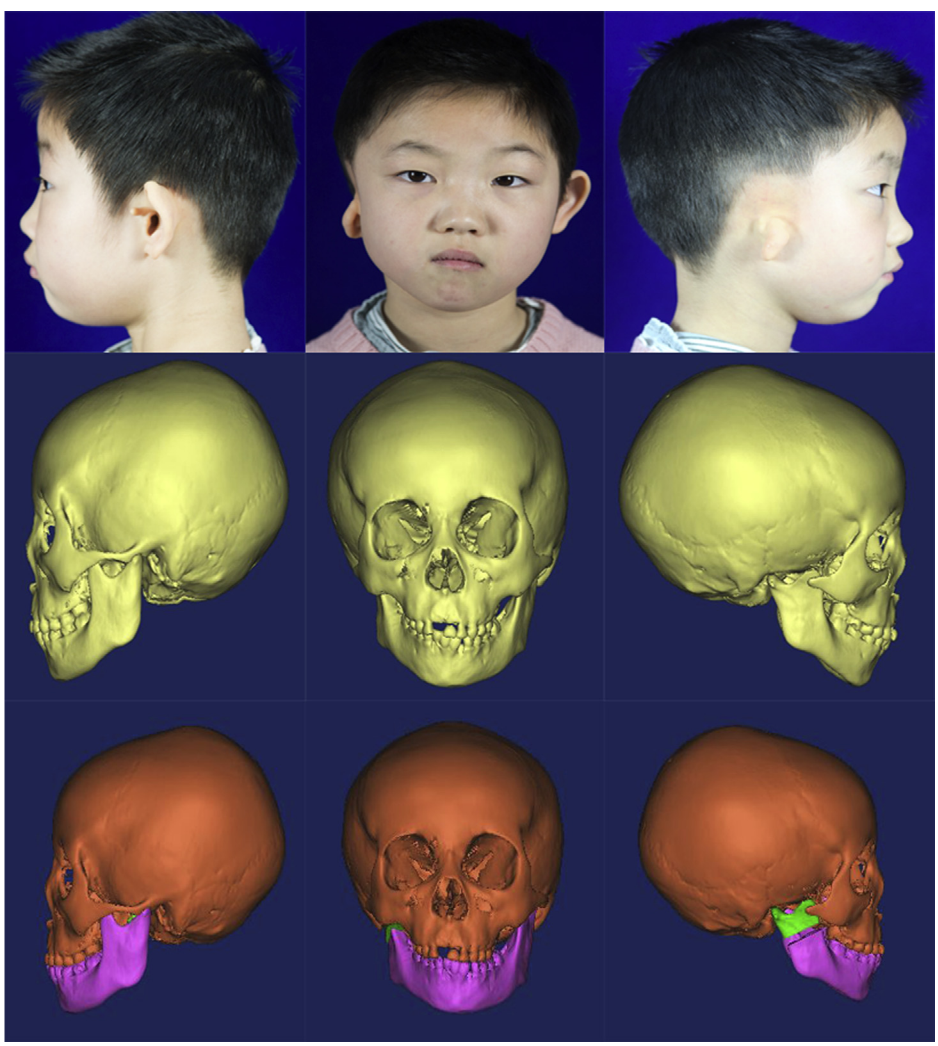

Fig. 15. The first row shows preoperative pictures of a 5-year-old female with right HFM, $O_3M_{2A}E_3N_4S_1$ classification, with a type M2A mandible. The second row shows preoperative 3D models formed using MIMICS V18. The third row shows a computer-simulated plan of the distraction process. The simulation was designed to move the pogonion to the sagittal line (midfacial line). Vertical distraction of the mandibular ramus was applied in order to achieve this target.

direction. The influence of experience also became a barrier in vector selection.

The virtual surgical planning proved accurate in terms of improving intercondylar distance, height of mandibular ramus, length of mandibular body, width of mandible, and angle of affected mandible. For each type of OMENS-plus classification, the comparison between postoperative data and virtual surgical planning data proved to be highly accurate for height of mandible, but less accurate for length. This limitation may be due to the unidirectional distraction — in types M2A–M2B the mandible is deformed and deficient in both vertical and horizontal directions. For type M3 cases, we were able to provide the basis of a mandibular ramus for temporomandibular joint reconstruction surgery.

Figs. 15 and 16 show the oral commissure from patient No. 1 before surgery and after surgery. Surgical simulation planning in this case showed improvement of the occlusal plane and mandibular shape after distraction osteogenesis by surgical simulation planning, however, the surgeon performed overcorrection due to the growth. The computer simulated movement of the pogonion to the sagittal or midfacial plane. The result of the distraction process matched the simulated plan exactly.

Figs. 17 and 18 show differing results for patient No.2. Good results for increase in height were achieved, but the length increase did not compare accurately with the computer planning. Sun et al. found a significant difference in intercondylar distance between the simulated and actual groups in patients undergoing unidirectional mandibular distraction osteogenesis, which was caused by an error in CAD/CAM (Sun et al., 2013) resulting from pseudoarthrosis of the coronoid process between the affected mandible and the base of the skull. Meanwhile, Paeng et al. proposed simulation based on the rotational movement of the mandible on the axis passing through the condylar head of the non-affected side (Paeng et al., 2007). Troulis et al. suggested that the coronoid may collide with the base of the skull before agenesis of the condylar processes while the hypoplastic condyle remains disarticulated (Troulis et al., 2002).

Surgical simulation planning on the affected side of the mandible requires meticulous analysis of the three dimensional movement of the distracted mandibular segment. Hopper et al. studied distal movement of the mandible during a distraction osteogenesis process working at 1 mm per day (Hopper et al., 2006). This method is not cost effective due to the lavish equipment required for monitoring the process. The distal segment does not move until the distracted proximal segment reaches the base of the skull and forms a pseudoarthrosis. Pseudoarthrosis will change the predetermined rotational point, thus affecting the accuracy of the prediction. This explains why the accuracy of several predictive methods remains a controversy. We tend to remove the coronoid segment of the affected mandible in order to achieve the predicted results.

In a recent study, Steinbacher et al. sought to determine whether mandibular deformity in HFM resulted in a volumetric deficiency in the ramus–condyle unit (Steinbacher et al., 2011). To evaluate the mandibular deformity in this manner, 3D-rendered volume segments were analyzed using a surgical planning program (CMF, Materialize, Leuven, Belgium). These results where then compared with the current Pruzansky classification system. The 3D images of mandibles were split into hemimandibles using the midline, and then each hemimandible was divided into dentate and proximal segments. The volumes of affected and unaffected hemimandibles and segments were then compared with controls. As expected, the results showed that the hemimandible and proximal segments of the affected side had reduced volumes compared with the unaffected side. However, the dentate segment on the affected side also showed a reduced volume. They also found that the

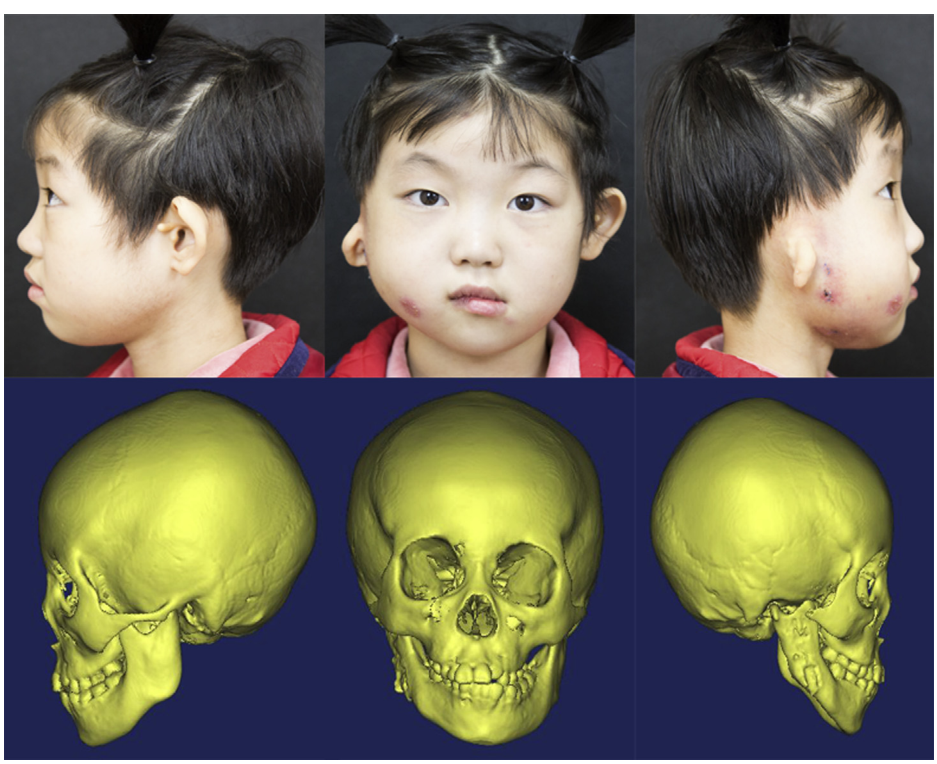

Fig. 16. The first row shows postoperative images taken 2 weeks after removal of the intraoral distraction device. The second row shows that the desired outcome was achieved, with equal ramus height in both the affected and non-affected mandible, with the pogonion aligned with the sagittal (midfacial) plane, as planned.

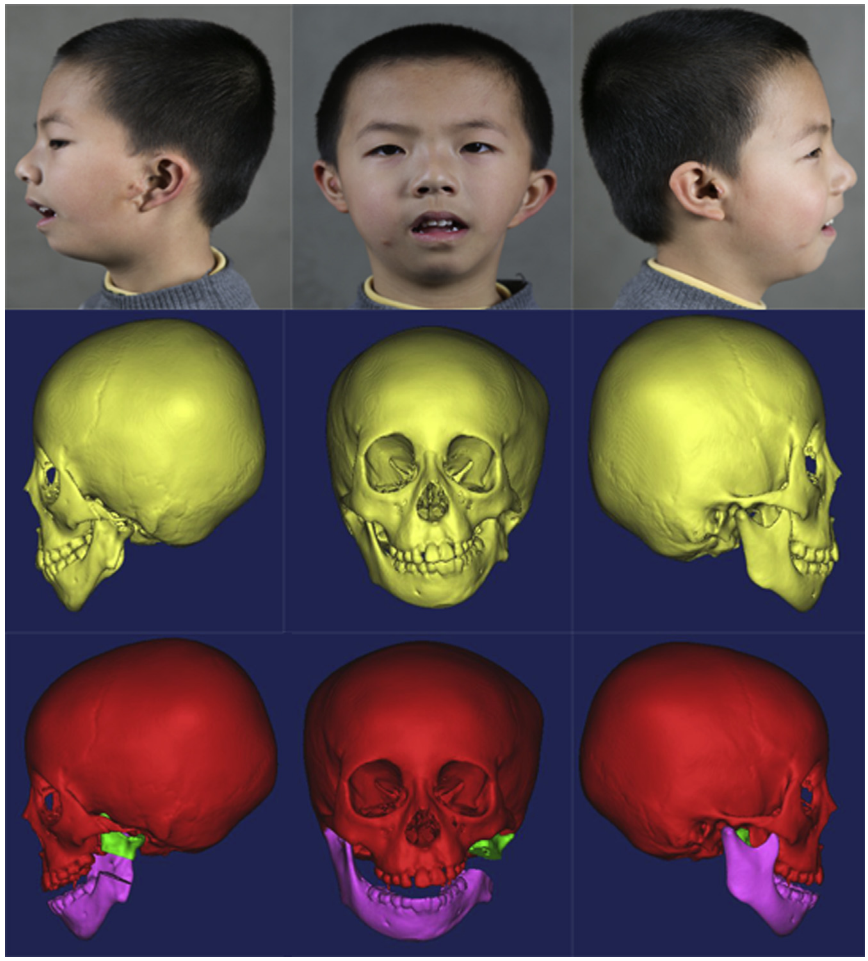

Fig. 17. The first row shows preoperative images of a 7-years-old with left HFM, $O_1M_{2B}E_1N_0S_2$ classification, with a type M2B mandible. The second row shows preoperative 3D models formed using MIMICS V18. Differences in height and length are evident between the affected and non-affected sides. The third row shows a computer-simulated plan of the distraction process and simulation of results. The distraction process aimed to move the pogonion to the sagittal or midfacial line.

Fig. 18. The first row shows postoperative images taken 2 weeks after removal of the intraoral distraction device. The second row shows postoperative 3D models, with the pogonion shifted to the midfacial line. The pseudoarthrosis formed between the coronoid process of the affected side and the base of the skull, which resulted in deviation from the computer-simulation results.

unaffected side was smaller than the controls, which demonstrates the bilateral nature of HFM. The study also verified an inverse relationship between the severity of Pruzansky score and mandibular volume for both the proximal mandibular segment and the total hemimandible. This study proved objectively that the dentate and proximal segments were significantly affected in HFM.

Computer simulation planning is a specialist technology that has brought simplicity, predictability, and accuracy. However, there are barriers to its implementation. Each center needs substantial funds just to fulfill the basic requirements of this technique. Expensive software (MIMICS V15 and 3-Matic V7, Materialise, Leuven, Belgium), a top-of-the-range 3D printer (Project 660 Pro, 3Dsystems, USA), and highly paid engineers were essential to complete this study. Such factors make this new technology less applicable for small craniofacial centers, or even for developing countries.

6. Conclusion

3D technology has turned the seemingly impossible into reality. For example, the time required for surgery has reduced, and the outcome has become more predictable. For HFM cases, this therapeutic strategy can be planned for any classification of severity. The distraction process can even be monitored over a certain period of time, without the child requiring the repeated doses of radiation associated with serial cephalogram radiography.

Authors' contributions

Andy **Tan**,M.D.-Analysis and interpretation of the data, draft the article
Yuanhao **Chai**-Acquisition of the data and measurements
Weijun **Mooi**,M.D.-Acquisition of the data
Xiaojun **Chen**,M.D.-Completion of the Measurement and acquisition of the data
Haisong **Xu**,M.D.-Participate in the operation
Mar Aung **Zin**,M.D.-Participate in the operation
Li **Lin**,M.D.-Participate in the operation
Yan **Zhang**, M.D.-Design the implementation plane
Xianxian **Yang**,M.D.-Guidance of the task and revision of the article
Gang **Chai**,M.D.-The overall arrangements and revision of the article

Financial disclosure statement

Financial support was provided by the Three-Year plan for Promoting Clinical Skills and Clinical Innovation in Municipal Hospitals, Hospital Development Center, Shanghai (16CR2010A), and the Clinical Research Program of the Ninth People's Hospital, Shanghai Jiao Tong University School of Medicine (JYLJ031). The authors have no financial interest in any of the products or devices mentioned in this article.

Appendix A. Supplementary data

Supplementary data to this article can be found online at https://doi.org/10.1016/j.jcms.2018.11.014.

References

Altobelli DE, Kikinis R, Mulliken JB, Cline H, Lorensen W, Jolesz F: Computer-assisted three-dimensional planning in craniofacial surgery. Plast Reconstr Surg 92(4): 576–585, 1993
Cavalcanti MG, Rocha SS, Vannier MW: Craniofacial measurements based on 3D-CT volume rendering: implications for clinical applications. Dentomaxillofac Radiol 33(3): 170–176, 2004
Dec W, Peltomaki T, Warren SM, Garfinkle JS, Grayson BH, McCarthy JG: The importance of vector selection in preoperative planning of unilateral mandibular distraction. Plast Reconstr Surg 121: 2084–2092, 2008
Eufinger H, Wehmöller M, Machtens E, Heuser L, Harders A, Kruse D: Reconstruction of craniofacial bone defects with individual alloplastic implants based on CAD/CAM-manipulated CT-data. J Craniomaxillofac Surg 23(3): 175–181, 1995
Gateno J, Xia JJ, Teichgraeber JF: A new three-dimensional cephalometric analysis for orthognathic surgery. J Oral Maxillofac Surg 68: 606–622, 2011
Grayson BG, Cutting C, Bookstein FL, Kim H, McCarthy JG: The three-dimensional cephalogram: theory, technique, and clinical application. Am J Orthod Dentofacial Orthop 94: 327–337, 1988
Grayson BH, McCormick S, Santiago PE, McCarthy JG: Vector of device placement and trajectory of mandibular distraction. J Craniofac Surg 8: 473–480, 1997
Grayson BH, Santiago PE: Treatment planning and vector analysis of mandibular distraction osteogenesis. Atlas Oral Maxillofac Surg Clin North Am 7(1–13), 1999
Hanson PR, Melugin MB: Orthodontic management of the patient undergoing mandibular distraction osteogenesis. Semin Orthod 5(1): 25–34, 1999
Hopper RA, Grayson BH, Dayan J, Altug A, McCarthy JG, Sato Y, et al: A virtual reality tracking system for distal mandible movement during distraction osteogenesis. Plast Reconstr Surg 117(2): 590–594, 2006
Lo LJ, Marsh JL, Vannier MW: Craniofacial computer assisted surgical planning and simulation. Clin Plast Surg 21: 501–516, 1994
McCarthy JG, Schreiber J, Karp N, Thorne CH, Grayson BH: Lengthening the human mandible by gradual distraction. Plast Reconstr Surg 89(1–10), 1992
McCarthy JG, Stelnicki EJ, Mehrara BJ, Longaker MT: Distraction osteogenesis of the craniofacial skeleton. Plast Reconstr Surg 107: 1812–1827, 2001
Paeng JY, Lee JH, Lee JH, Kim MJ: Condyle as the point rotation for 3-D planning of distraction osteogenesis for hemifacialmicrosomia. J Cranio-Maxillofac Surg 35(2): 91–102, 2007
Steinbacher DM, Gougoutas A, Barlett SP: An analysis of mandibular volume in hemifacial microsomia. Plast Reconstr Surg 127(6): 2407–2412, 2011
Sun H, Li B, Zhao Z, Zhang L, Shen SG, Wang X: Error analysis of a CAD/CAM method for unidirectional mandibular distraction osteogenesis in the treatment of hemifacial microsomia. Br J Craniomaxillofac Surg 51(8): 892–897, 2013
Troulis MJ, Everett P, Seldin EB, Kikinis R, Kaban LB: Development of a three dimensional treatment planning system based on computed tomographic data. Int J Oral Maxillofac Surg 31(4): 349–357, 2002